The Soil, Vegetation, and Snow land surface scheme

The Interactions between Surface, Biosphere, and Atmosphere (ISBA) scheme has been used operationally at the Meteorological Service of Canada (MSC) since 2001 for the prognostic evolution of land surface variables (temperature, soil moisture, snow) and to provide fluxes of heat, water, and momentum in the Global Environmental Multi-scale (GEM) model (Bélair et al. 2003a,b, 2009). Throughout these years, several weaknesses have been identified in the representation of land surface processes with ISBA, but were not corrected due to the scheme's operational status (which always makes it difficult to change physical parameterizations). In this document, a new land surface scheme is documented. This scheme, called the Soil, Vegetation, and Snow (SVS) scheme, is developed and tested as a replacement to ISBA in MSC's operational numerical environmental prediction applications.

The main features of SVS are the following, as compared with ISBA:

- energy and water budgets for vegetation, two snow packs, and ground underneath vegetation and snow (with new tiling approach);
- improved parameterization of the vegetation thermal coefficient;
- inclusion of photosynthesis process in order to evaluate the surface stomatal resistance;
- new formulations for land surface albedo and emissivity;
- new snow pack under the vegetation;
- root density function depending on the vegetation type;
- multi-layer water vertical transport in the soil;
- representation of freeze/thaw (F/T) state for each soil layer;

These modifications, along with the rest of SVS, are described and discussed below.

A. Land surface prognostic variables and parameters

The number of prognostic variables has been substantially increased in SVS, as shown in this list:

- T_{GS}: surface temperature of bare ground (K),
- T_{Gd}: surface mean temperature of bare ground (K),
- T_{VS}: surface temperature of vegetation canopy (K),
- T_{Vd}: mean surface temperature of vegetation canopy (K),
- T_{SNS}: surface temperature of snow over low or non-vegetated areas (K),
- T_{SNd}: mean surface temperature of snow over low or non-vegetated areas (K),

- T_{SVHS}: surface temperature of snow under high vegetation (K),
- T_{SVHd}: mean surface temperature of snow under high vegetation (K),
- W_{SSN}: snow mass over low or non-vegetated areas (kg m^{-2}),
- W_{SSVH}: snow mass under high vegetation (kg m^{-2}),
- W_{LSN}: liquid water in the snow pack over low or non-vegetated areas (kg m^{-2}),
- W_{LSVH}: liquid water in the snow pack under high vegetation (kg m^{-2}),
- α_{SN}: albedo of the snow pack over low or non-vegetated areas,
- α_{SVH}: albedo of the snow pack under high vegetation,
- ρ_{SN}: density of the snow pack over low or non-vegetated areas (kg m^{-3}),
- ρ_{SVH}: density of the snow pack under high vegetation (kg m^{-3}),
- $w_{(n)}$: liquid volumetric soil moisture content for each soil layer (m^3 m^{-3}),
- $w_{f(n)}$: solid volumetric soil moisture content for each soil layer (m^3 m^{-3}),
- W_r: liquid water in the vegetation canopy (kg m^{-2}).

The following land surface parameters have to be provided to SVS:

- z_{0m}: roughness length for momentum turbulent transfers representative of the entire model grid cell area (m)
- z_{0m_local}: roughness length for momentum turbulent transfers, including only the vegetation component (m)
- v_{low}: fractional coverage of low vegetation (grass, crops, shrubs) over land,
- v_{high}: fractional coverage of high vegetation (forests) over land,
- *LAI*: total leaf area index over vegetation area of the land surface (m^2 m^{-2}),
- LAI_{vh}: leaf area index over high-vegetation area of the land surface (m^2 m^{-2}),
- *sand*: sand fraction of soil (%),
- *clay*: clay fraction of soil (%),
- d_{rz}: root-zone depth (m),
- *B*: form parameter for subgrid-scale surface flow (or runoff),
- $\alpha_{g\_WS:}$ bare ground broadband white-sky (diffused radiation) albedo for visible and near-infrared,
- $\alpha_{g\_BS:}$ bare ground broadband black-sky (direct radiation) albedo for visible and near-infrared,
- $\alpha_{veg\_WS:}$ vegetation broadband white-sky (diffused radiation) albedo for visible and near-infrared,
- $\alpha_{veg\_BS:}$ vegetation broadband black-sky (direct radiation) albedo for visible and near-infrared,
- ε_V: vegetation emissivity.

B. Tiling approach

As is the case for ISBA, the SVS surface scheme is used to calculate surface fluxes over land only. Surface fluxes (and more generally physical processes) over sea-ice,

glaciers, cities, and water bodies are addressed by other sets of parameterizations within the surface modeling system.

The tiling approach has been substantially modified in SVS compared with ISBA in order to calculate energy budgets for (a) bare ground, (b) vegetation, (c) ground under the vegetation, (d) snow covering bare ground and low vegetation, and (e) snow covering the ground under high vegetation. Land cover fractions are modified in SVS in order to accommodate the multiple energy budgets. Figure 1 illustrates the new land surface tiling approach.

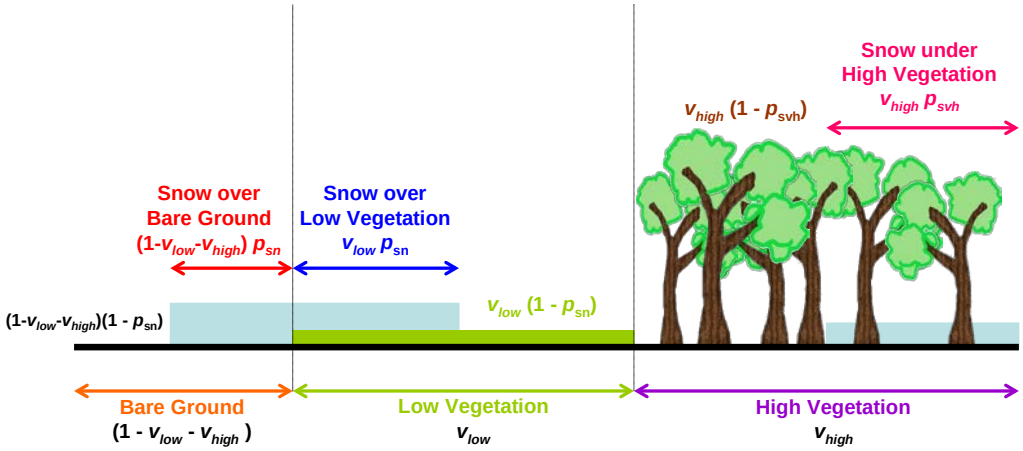

Fig1. Land Surface Tiling Approach In Multibudget ISBA

In this figure, v_{low} is the fraction of low vegetation over land, v_{high} is the fraction of high vegetation over land, p_{svh} is the fraction of snow under high vegetation, and p_{sn} is the fraction of snow covering low vegetation or bare ground.

The land surface tiling is done in two steps. First the land tile is divided into (1) bare ground, (2) low vegetation, and (3) high vegetation fractions, adding up to a hundred percent. These three land cover types are then further split into a snow or no-snow areas, with corresponding fractions. The high vegetation is distinguished from low vegetation in a pre-processor, and both fractions are provided as input to SVS based on the vegetation type. If a particular vegetation type is deemed to be high enough *not* to be covered by snow (i.e., forests), it is considered to be "high", otherwise it is specified as "low". The remainder of the land, i.e., $\left(1 - v_{low} - v_{high}\right)$, is considered as bare ground.

In SVS, it is assumed that the snow pack overlaying bare ground and low vegetation evolves as one, with the associated snow cover fraction equal to

$$p_{sn} = \min\left(\frac{W_s}{W_{crn}}, 1.0\right) \tag{1}$$

where W_s is the snow mass or the equivalent water content of the snow reservoir (kg m^{-2}), and W_{crn} = 10 kg m^{-2}. The snow pack under the high vegetation evolves separately, and the associated snow cover fraction (p_{svh}) is given by a similar equation:

$$p_{svh} = \min\left(\frac{W_{svh}}{W_{crn}}, 1.0\right) \tag{2}$$

where W_{svh} is the equivalent water content of the snow under high vegetation (SVH subscript) reservoir (kg m^{-2}). It should be noted that the spatial fraction in (2) represents the snow fraction under high vegetation as seen from the "ground". To compute the snow fraction under high vegetation as seen from space or from the atmosphere (p_{svh_a}), the ground fraction p_{svh} must be modified to account for the shielding effect of leaves following:

$$p_{svh\_a} = \max\left(LAI_0 - LAI'_{vh}, 0.0\right) p_{svh} \tag{3}$$

where $LAI'_{vh} = \max(LAI_{vh}, f_{wood})$ to account for the effect of the woody portions of forests (f_{wood} = 0.1 for forests, and f_{wood} = 0 for other land uses), LAI_{vh} is the leaf area index (LAI) of high vegetation (m^2 m^{-2}) and, LAI_0 is a threshold value of leaf area index (1.0 m^2 m^{-2} is used here).

Given the above, the land portion of each model grid area is partitioned based on the following fractions:

- bare ground:

$$\left(1 - v_{low} - v_{high}\right)\left(1 - p_{sn}\right) \tag{4}$$

- vegetation (low and high):

$$v_{low}\left(1 - p_{sn}\right) + v_{high}\left(1 - p_{svh}\right) \tag{5}$$

- snow (excluding snow under vegetation):

$$p_{sn}\left(1-v_{low}-v_{high}\right)+p_{sn}v_{low}=p_{sn}(1-v_{high}) \tag{6}$$

- snow under high vegetation:

$$p_{svh}v_{high}\,. \tag{7}$$

From the atmosphere, however, the vegetation fraction is $v_{low}\left(1-p_{sn}\right)+v_{high}\left(1-p_{svh\_a}\right)$, while the snow under high vegetation fraction is $p_{svh\_a}v_{high}$.

C. Vertical layering in SVS

Another major difference with ISBA is related to the vertical layering, or vertical discretization, used in SVS for the different surface components. As shown in Fig. 2, SVS considers a single-layer vegetation canopy for which the Force-Restore (FR) equations are used for the evolution of instantaneous and mean canopy temperatures. For the ground portion, two single-layer snow packs can be represented over bare soil and under the high vegetation. In the SVS FR version (as presented in this document), the snow temperature evolves according to the FR equations, as in ISBA. The forcing being different over bare soil and under the vegetation, the two snow packs evolve differently.

In the soil, a set of layers of a predefined number N_L is used. Soil moisture is represented in each of these layers based on vertical transport, evapotranspiration, and surface / lateral flows. In this first version of SVS (presented in this document), soil temperature is defined only at the soil surface and its evolution is based on a simple approach. In future SVS versions, soil temperature will be defined at the interface of each of the soil layer, and will evolve based on vertical heat transport and phase changes, with a closure at the surface based on energy budgets for all the land sub-tiles, including bare soil as well as soil under vegetation and under snow (with and without vegetation). Thus, several soil temperature profiles will be represented in SVS. This more sophisticated version of SVS will allow for the representation of F/T processes for each soil layer. When present, the single snow layer will be part of the numerical solution of the vertical diffusion of heat in SVS.

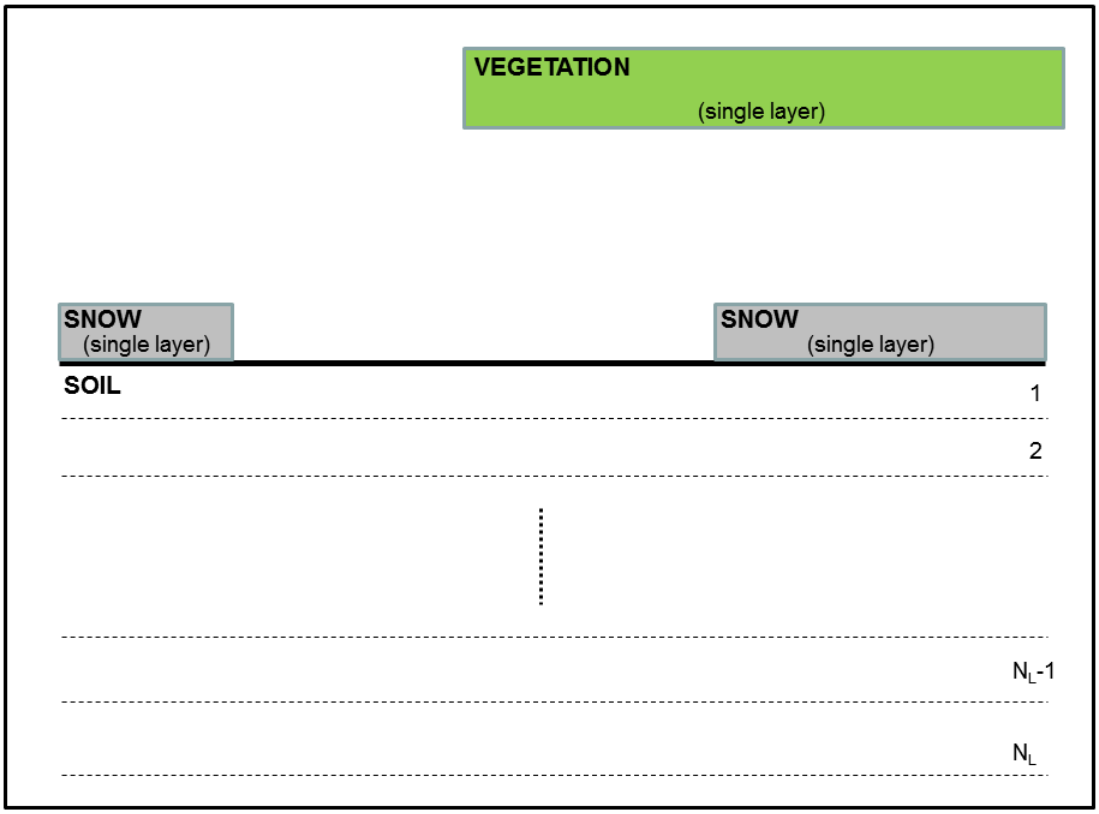

Figure 2. Vertical discretizations of the various surface components in SVS.

D. Vegetation

In SVS, a single energy budget is calculated for all types of vegetation. The physical properties of the vegetation canopy are calculated using a weighted mean based on the fraction of coverage of each vegetation type. The prognostic equations for the superficial and mean vegetation temperatures (T_{Vs} and T_{Vd}) are obtained from the FR method:

$$\frac{\partial T_{Vs}}{\partial t} = C_V'(R_V - H_V - LE_V) - \frac{2\pi}{\tau}(T_{Vs} - T_{Vd}) \tag{8}$$

$$\frac{\partial T_{Vd}}{\partial t} = \frac{1}{\tau}(T_{Vs} - T_{Vd}) \tag{9}$$

in which R_V, H_V, LE_V are the net radiation, sensible heat and latent heat fluxes over vegetation. Typically, the thermal coefficient C_V' is much larger than its counterpart C_G

for bare soil (Deardorff 1978, Dickinson 1984) because heat storage is much smaller in vegetation canopy than in the ground.

The thermal coefficient C_V' has been modified for vegetation (compared with what is done in ISBA) to take into account the contribution of the bare ground visible through the vegetation canopy; it is written as:

$$C_V' = \frac{\min(LAI', LAI_0)}{LAI_0} C_V + \frac{\max(LAI_0 - LAI', 0.0)}{LAI_0} C_{noleaf} \tag{10}$$

where $LAI' = \max(LAI, f_{wood})$ to account for the effect of woody portions of forests, *LAI* is the aggregated value (m^2m^{-2}), LAI_0 still has a reference value of 1.0 m^2m^{-2}, C_V is the heat capacity of vegetation canopy (same values for all types of vegetation, chosen to be larger than in ISBA: $C_V = 4.x10^{-5}$ K m^2 J^{-1}, double of what is used in ISBA), and C_{noleaf} is the thermal coefficient for the leafless portion of the vegetation area

$$C_{noleaf} = \frac{v_{low}\left((1-p_{sn})C_g + p_{sn}C_{SN}\right) + v_{high}\left((1-p_{svh})C_g + p_{svh}C_{SVH}\right)}{v_{low} + v_{high}} \tag{11}$$

where C_{SN} and C_{SVH} are the thermal coefficients of the snow and snow-under-vegetation packs.

The net radiation at the canopy surface is given by:

$$R_v = \left\{F_{SS}^- - \alpha_{V\_WS}F_{SS\_WS}^- - \alpha_{V\_BS}F_{SS\_BS}^-\right\} + \varepsilon_V(F_{SI}^- - \sigma_{SB}T_{Vs}^4) \tag{12}$$

where ε_V is the aggregated vegetation emissivity and α_{V_WS} , α_{V_BS} are the white-sky and black-sky albedos for vegetation. All these quantities are provided as input to SVS. The sensible heat flux over vegetation is given by:

$$H_V = \frac{\rho_a c_p (T_{Vs} - T_a)}{RESA_V} \tag{13}$$

where $RESA_v$ is the aerodynamical surface resistance for the vegetation given by $(C_{Hv}V_a)^{-1}$ with C_{Hv} being the drag coefficient for heat over vegetation. The latent heat of evaporation from vegetation is $LE_V = \rho_a L_V E_V$, where E_V is the vegetation vapor flux provided by:

$$E_V = \frac{\overbrace{\left(h_V\, q_{sat}\left(T_{Vs}\right)+\left(1-h_V\right)q_a\right)}^{Specific\ Humidity\ of\ Vegetation} - q_a}{RESA_V} = \frac{h_V\left(q_{sat}\left(T_{Vs}\right)-q_a\right)}{RESA_v} \tag{14}$$

in which h_V is the Halstead coefficient and $q_{sat}\,(T_{Vs})$ is the saturated specific humidity at temperature T_{Vs}. If the vapor flux is negative (*i.e.*, $q_{sat}\,(T_{Vs}) < q_a$) , it is assumed that a dew flux occurs at the potential rate and h_V is set to 1.0. When the vapor flux is positive (*i.e.*, $q_{sat}\,(T_{Vs}) > q_a$), the Halstead coefficient h_V is calculated as :

$$h_V = 1 - \frac{(1-\delta)\,r_c}{RESA_V + r_c} \tag{15}$$

in order to account for both direct evaporation of intercepted water and the transpiration from vegetation. In (15), r_c is the stomatal (canopy-surface) resistance, and δ is a function of the moisture content of the interception reservoir given by Deardorff (1978):

$$\delta = \frac{\min\left(W_r, W_{r\max}\right)}{-2LAI\ \min\left(W_r, W_{r\max}\right) + (1+2LAI)W_{r\max}} \tag{16}$$

in which W_r is the water content retained by the canopy, and W_{rmax} is a maximum value of W_r over which the water cannot be retained by the canopy (foliage), and as a result, runoff to ground underneath takes place. Following Dickinson (1984), W_{rmax} is proportional to the density of the canopy:

$$W_{r\,max} = 0.2\ LAI \tag{17}$$

The surface stomatal resistance is obtained from representation of photosynthesis processes, and is described in detail in section E. The root-zone profile follows Schenk and Jackson (2003), based on:

$$r(D) = \frac{1}{1+\left(\frac{D}{D_{50}}\right)^c} \tag{18}$$

in which *r(D)* is the fractional amount of roots (compared with the total amount of roots) above depth D (in cm), D_{50} is the depth at which 50% of roots are found above, and c is a shape parameter. By setting D_{50} = 50 cm, and by having D_{95} = 100 d_{rz}, then the shape parameter can be determined, i.e.,

$$c = \frac{Log\left(0.05 / 0.95\right)}{Log\left(\frac{100.\, d_{rz}}{50.}\right)} \tag{19}$$

in which d_{rz} is the depth of the root zone layer. The fractional roots amount in a specific layer n is given by:

$$f_{n,root} = r(n) - r(n\text{-}1) \tag{20}$$

As mentioned above, a positive vegetation vapor flux includes the contribution of both direct evaporation from the fraction of the foliage covered by intercepted water, and transpiration from the remaining part of the leaves. A negative vapor flux consists only of the dew flux, with the leave transpiration set to zero. Specifically, the transpiration flux E_{tr} is given by:

$$E_{tr} = \begin{cases} \dfrac{1-\delta}{RESA_V + r_c}\left(q_{sat}(T_{Vs}) - q_a\right) & if \quad q_{sat}(T_{Vs}) > q_a \\ 0. & if \quad q_{sat}(T_{Vs}) \le q_a \end{cases} \tag{21}$$

while the direct evaporation vapor flux E_d is simply the difference between the vegetation vapor flux and the transpiration flux:

$$E_d = E_v - E_{tr} \tag{22}$$

and the associated direct latent heat flux is given by $LE_d = \rho_a L_V E_d$.

E. Photosynthesis

A representation of photosyntesis processes is used to determined the surface stomatal resistance (or its inverse the stomatal conductance). In the photosynthesis model used in SVS both the effect of atmospheric CO_2 concentration and land-atmosphere CO_2 exchanges are taken into account. The SVS photosynthesis module is based on the biochemical approach (Farquhar et al., 1980; Collatz et al., 1991, 1992). It calculates intercellular CO_2 concentration c_i, net canopy photosynthesis rate, A_n ($\mu molCO_2 m^{-2} s^{-1}$), canopy leaf maintenance respiration (R_{mL}), and of course the stomatal resistance r_c (or conductance g_c). Both big-leaf and two-leaf (sunlit and shaded) approaches are included as options in SVS.

The gross photosynthesis rate (A_0) is co-limited by assimilation rates based on enzyme Rubisco (J_c), light (J_e) and transport capacity (J_s). The photosynthetic rate is limited by the photosynthetic Rubisco (J_c), and is written as:

$$J_c = V_m[\frac{c_i - \Gamma}{c_i + K_c(1+O_a/K_a)}] \quad \text{for C3 plants} \tag{23}$$

and

$$J_c = V_m \quad \text{for C4 plants} \tag{24}$$

where V_m (mol $CO_2\ m^{-2}s^{-1}$) is the temperature adjusted maximum catalytic capacity of Rubisco, c_i is the intercellular CO_2 concentration, O_a (Pa) is the partial pressure of atmospheric oxygen ($O_a = 0.2095p$), Γ is the CO_2 compensation point, p is the air pressure (Pa), and K_c and K_o (Pa) are the Michaelis-Menten constants for CO_2 and O_2, respectively. Also, V_m, Γ, K_c and K_o are all temperature dependent functions.

C3 and C4 refers to the carbon fixation metabolic pathways. C3 plants approximately represent 95% of the Earth's plant biomass, and thrive in regions with moderate sunlight and temperature, and with pleny of soil moisture. These plants lose 97% of the water gathered by their roots to evaporation. C4 plants are more recent in the World's history. This metabolic pathway is less frequent than for C3, but is more efficient in terms of water loss to the atmosphere. C4 plants include a large portion of grasses, as well as crops such as maize, sugar cane, and sorghum.

The gross photosynthetic rate limited by the light (J_e) is written as:

$$J_e = \alpha(1-\varpi)F_{PAR}[\frac{c_i - \Gamma}{c_i + 2\Gamma}] \qquad \text{for } C_3 \text{ plants} \tag{25}$$

$$J_e = \alpha(1-\varpi)F_{PAR} \qquad \text{for } C_4 \text{ plants} \tag{26}$$

where α is the quantum efficiency and values of 0.08 and 0.04 are used for C_3 and C_4 plants, respectively. Moreover, ϖ is the leaf scattering coefficient (with values of 0.15

and 0.17 are used for C_3 and C_4 plants, respectively) and F_{PAR} is the incident photosynthetically active radiation.

J_s represents the gross photosynthetic rate limited by the capacity to transport photosynthetic products for C_3 plants, but is the CO_2-limited capacity for C_4 plants.

$$J_S = 0.5V_m \qquad \text{for } C_3 \text{ plants} \tag{27}$$

$$J_S = 2\times 10^4 V_m \frac{c_i}{p} \qquad \text{for } C_4 \text{ plants} \tag{28}$$

Thus the gross photosynthetic rate at the top of canopy (A_0) is co-limited by J_c, J_e and J_s. To avoid a too-abrupt transition, these three limiting rates are combined into two quadratic equations (Collatz et al., 1991), the smaller root of which is then selected as A_0.

$$\beta_1 J_p^2 - J_p(J_c + J_e) + J_c J_e = 0 \tag{29}$$

$$\beta_2 A_0^2 - A_0(J_p + J_s) + J_p J_s = 0 \tag{30}$$

where J_p is the smoothed minimum of J_c and J_e. Values of 0.95 and 0.99 are used for the empirical constants, β_1 and β_2, respectively.

For the two-leaf model, J_c and J_s are estimated using the same equations as for the one-leaf model. A difference though is that scattering is included in calculating the light extinction parameter k_b (see below), and therefore the term $1-\varpi$ in (25) and (26) is omitted for the estimate of the gross photosynthetic rate limited by the light (J_e):

$$J_e = \alpha I[\frac{c_i - \Gamma}{c_i + 2\Gamma}] \qquad \text{for } C_3 \text{ plants} \tag{31}$$

$$J_e = \alpha I \qquad \text{for } C_4 \text{ plants} \tag{32}$$

where *I* is the diffused fraction of PAR for the shaded part of the canopy and is the direct beam fraction for the sunlit part.

The CO_2 compensation point Γ in (23) to (26) for C_3 and C_4 plants is based on:

$$\Gamma = \frac{O_a}{2\sigma} \qquad \text{for C3 plants} \tag{33}$$

$$\Gamma = 0 \qquad \text{for C4 plants} \tag{34}$$

in which σ is Rubisco: $\sigma = 2600.0\, f_{25}(0.57)$, and f_{25} is the standard Q_{10} temperature function $f_{25}(Q_{10}) = Q_{10}^{\,0.1(T_{Vd}-25)}$.

The Michelis-Menton constants for CO_2 (K_c) and O_2 (K_o) in (23)-(24) are given by

$$\begin{aligned} K_c &= 30\, f_{25}(2.1) \\ K_o &= 3\times 10^4\, f_{25}(1.2) \end{aligned} \tag{35}$$

and the temperature-adjusted maximum catalytic capacity of Rubisco, V_m, used in (23)-(24) and (27)-(28) is given by:

$$V_m = \frac{V_{\max} f_{25}(2.0)}{[1+\exp\{0.3(T_c - T_{up})\}][1+\exp\{0.3(T_{low} - T_{Vd})\}]} \tag{36}$$

where $V_{\max}$ is the maximum Rubisco capacity and is specified as an input parameter in photosynthesis subroutine, T_{Vd} is canopy temperature, and T_{up} and T_{low} are temperature thresholds which are taken as vegetation dependent constants.

The photosynthesis rate at leaf level (A_0) modeled by describing the co-limitation effect of J_c, J_e and J_s is then scaled up from leaf to canopy based on the assumption that the profile of leaf nitrogen content through the depth of the canopy follows the time-mean profile of radiation (Sellers et al., 1992). Similar to the scaling up of F_{PAR} to canopy ($f_{scale} = \frac{1}{k_n}(1 - e^{-k_n L_T})$) in the big-leaf model the photosynthesis rate at leaf level, A_0, is scaled up to canopy (A_{canopy}) by:

$$A_{canopy} = A_0 \frac{1 - e^{-k_n LAI}}{k_n} \tag{37}$$

in which k_n is a vegetation-dependent nitrogen extinction coefficient.

In the two-leaf model the canopy is divided into sunlit and shaded fractions for which the photosynthesis rates are estimated separately. The photosynthesis rates over

the depth of the canopy for sunlit (A_{sun}) and shaded (A_{sha}) fractions of the canopy are described as:

$$A_{sun} = A_{0,sun} \frac{(1 - e^{-(k_n + k_b)LAI})}{(k_n + k_b)} \tag{38}$$

$$A_{sha} = A_{0,sha} \left(\frac{1 - e^{-k_n LAI}}{k_n} - \frac{1 - e^{-(k_n + k_b)LAI}}{k_n + k_b}\right) \tag{39}$$

where k_b is the light extinction parameter and is written as functions of cosine of solar zenith angle (μ) and leaf scattering coefficient (ϖ) (Sellers ,1985):

$$k_b = \frac{G(\mu)}{\mu}(1 - \varpi)^{\frac{1}{2}} \tag{40}$$

$$G(\mu) = \phi_1 + \phi_2 \mu \tag{41}$$

$$\phi_1 = 0.5 - 0.663\chi - 0.33\chi^2 \tag{42}$$

$$\phi_2 = 0.877(1 - 2\phi_1) \tag{43}$$

where χ is an empirical vegetation-dependent parameter describing leaf angle distribution (values between -0.4 and 0.6). The total canopy photosynthesis for two-leaf model is then obtained by adding A_{sun} and A_{sha}.

Most vegetative canopies suffer from soil water stress when soil moisture is low. The effect of soil water stress on photosynthetic rate (A_{canopy}) is given by

$$A_{canopy,stressed} = A_{canopy} G(w_{soil}) \tag{44}$$

The soil moisture stress term, $G(\theta)$, is given by

$$G(w_{soil}) = 1.0 - (1.0 - \beta)^n, \quad n = 2 \tag{45}$$

$$\beta(w_{soil}) = \max[0, \min[1, \frac{w_{soil} - w_{wilt}}{w_{fc} - w_{wilt}}]] \tag{46}$$

where β is the degree of soil saturation, w_{soil}, w_{wilt} and w_{fc} are the soil moisture content, wilting point soil moisture and field capacity, respectively. The soil moisture stress $G(w_{soil})$ is calculated for all soil layers and then weighted according to the root fraction in each layer.

Finally, the net canopy photosynthesis rate, A_n ($\mu molCO_2 m^{-2} s^{-1}$) is calculated to estimate canopy conductance:

$$A_n = A_{canopy,stressed} - R_{mL} \tag{47}$$

where R_{mL} is canopy leaf maintenance respiration, which is written as

$$R_{ml} = 0.015 A_{canopy} \quad \text{for C3 plants} \tag{48}$$

$$R_{ml} = 0.025 A_{canopy} \quad \text{for C4 plants} \tag{49}$$

Studies have shown that during daytime R_{mL} is less sensitive than photosynthesis to air temperature (Pons and Welschen, 2003; Xu and Baldocchi, 2003).

In SVS, formulations from Ball et al. (1987) and from Leuning (1995) can be used to evaluate the canopy conductance, g_c ($\mu CO_2 m^{-2} s^{-1}$. The Ball et al. stomatal conductance is given by,

$$g_c = m \frac{A_n h_s p}{c_s} + b\, LAI \tag{50}$$

where h_s is the relative humidity, and c_s is partial pressure of CO_2 at the leaf surface (Pa). Both *m* and *b* are vegetation dependent parameters.

Leuning (1995) on the other hand uses the vapor pressure deficit instead of relative humidity to calculate g_c, which is written as,

$$g_c = m \frac{A_n p}{(c_s - \Gamma)} \frac{1}{(1 + D/D_0)} + b\, LAI \tag{51}$$

where *D* is air vapor pressure deficit (Pa), D_0 is a vegetation dependent parameter (Pa).

The CO_2 partial pressure at the leaf surface, c_s, used in Ball et al. (1987) and Leuning (1995) formulations is obtained from

$$\frac{c_a - c_s}{p} \frac{g_b}{1.4} = A_n \tag{52}$$

The aerodynamic conductance, g_b, is obtained from the land surface model as an input. The intercellular CO_2 concentration, c_i, used in calculating assimilation rates in (23)-(28) is also estimated by net canopy photosynthesis rate, A_n,

$$\frac{c_s - c_i}{p}\frac{g_c}{1.6} = A_n \tag{53}$$

In SVS, intercellular CO_2 concentration, C_i, is used to find the value of canopy photosynthesis rate, A_n, which is then used to calculate intercellular CO_2 concentration. This cycle is repeated in an iterative process, with four iterations performed every time step.

Finally, the stomatal resistance is simply written as,

$$r_c = \frac{1}{g_c} \tag{54}$$

This stomatal resistance is then used for the calculation of evapotranspiration, as described in the previous subsection.

F. Bare ground

The prognostic equations for the superficial and mean bare ground temperatures (T_{Gs} and T_{Gd}) are obtained from the FR method, as proposed by Bhumralkar (1975) and Blackadar (1976):

$$\frac{\partial T_{Gs}}{\partial t} = C_g(R_g - H_g - LE_g) - \frac{2\pi}{\tau}(T_{Gs} - T_{Gd}) \tag{55}$$

$$\frac{\partial T_{Gd}}{\partial t} = \frac{1}{\tau}(T_{Gs} - T_{Gd}) + C_g L_f(freez_g - melt_g) \tag{56}$$

where t stands for time, C_g is the thermal coefficient for bare ground, R_g, H_g, LE_g are the net radiation, sensible heat and latent heat fluxes over bare ground respectively, L_f is the latent heat of fusion, $freez_g$ and $melt_g$ are fluxes of freezing and melting soil water, and τ is a time constant equal to one day. The thermal coefficient of bare ground is given by:

$$C_g = C_{gsat}\left(\frac{w_{sat}}{\max(w_{\text{int}} + w_{f\,\text{int}}, 0.001)}\right)^{b/2\ln 10} \quad ; \quad C_g \le 2.0\times10^{-5}\,\text{Km}^2\text{J}^{-1} \tag{57}$$

where C_{gsat} is the soil thermal coefficient at saturation, w_{sat} is the saturation soil moisture volumetric content, w_{int} is the soil moisture volumetric content for an intermediate soil layer (chosen here as about 10 cm, which corresponds to the two top soil layers), w_{fint} is the volumetric water content of frozen soil water in the same soil layer, and b is the slope

of the retention curve (Noilhan and Planton 1989). The soil thermal properties are obtained from the sand and clay fractions. The net radiation over bare ground is given by:

$$R_g = \left\{F_{SS}^{-} - \alpha_{g\_WS} F_{SS\_WS}^{-} - \alpha_{g\_BS} F_{SS\_BS}^{-}\right\} + \varepsilon_g (F_{SI}^{-} - \sigma_{SB} T_{Gs}^4) \quad (58)$$

Where F_{SS}^{-}, F_{SI}^{-} are the total incoming solar and infrared radiation, $F_{SS\_BS}^{-}, F_{SS\_WS}^{-}$ are the incoming direct / diffuse solar and infrared radiation at the surface, α_{g_WS} and α_{g_BS} are the white-sky (diffuse) and black-sky (direct) albedos for bare ground, ε_g is the bare ground emissivity, and σ_{SB} is the Stefan-Boltzmann constant. The bare ground albedo is provided as an input to SVS, based on land use / land cover classification and possibly on space-based remote sensing information (e.g., MODIS). Without going into all the relatively complex details of the specification of the bare ground albedo (which involves some downscaling and comparison with NDVI products), it can be mentioned that bare ground albedo (and emissivity) can be determined based on the sand and clay fraction in the soil, as well as the soil wetness. A bi-linear approach is used to interpolate between the albedo / emissivity values of four "extreme" soil types: dry-sand, wet-sand, dry-clay and wet-clay. These values are listed in Table 1 below.

Table 1. Albedo and emissivity values for soil types based on *Handbook of Soil Science, M.E. Summer, 2000.*

Soil Type	Albedo	Emissivity
dry sand	0.35 ($\alpha_{drysand}$)	0.95 ($\varepsilon_{drysand}$)
wet sand	0.24 ($\alpha_{wetsand}$)	0.98 ($\varepsilon_{wetsand}$)
dry clay	0.15 ($\alpha_{dryclay}$)	0.95 ($\varepsilon_{dryclay}$)
wet clay	0.08 ($\alpha_{wetclay}$)	0.97 ($\varepsilon_{wetclay}$)

The bare ground albedo and emissivity are thus:

$$\alpha_g = \alpha_{drysand} A(1-SWI) + \alpha_{dryclay}(1-A)(1-SWI) + \alpha_{wetsand} A\,SWI + \alpha_{wetclay}(1-A)\,SWI \quad (59)$$

$$\varepsilon_g = \varepsilon_{drysand} A(1-SWI) + \varepsilon_{dryclay}(1-A)(1-SWI) + \varepsilon_{wetsand} A.SWI + \varepsilon_{wetclay}(1-A).SWI \quad (60)$$

in which $A = sand/(sand + clay)$ and $SWI = (w_1 - w_{1\_wilt})/(w_{1\_sat} - w_{1\_wilt})$ is the soil wetness index for the near-surface soil layer, where w_1 is the soil moisture content for the first soil layer (typically of 5 cm depth) and w_{1_wilt} is the soil water content at the wilting

point for this same layer. It should be noted that the topsoil layer can dry past the wilting point or become supersaturated, but *SWI* must be constrained to the [0,1] range (*A* is in this range by construction).

The sensible heat flux over bare ground is:

$$H_g = \frac{\rho_a c_p (T_{Gs} - T_a)}{RESA_g} \tag{61}$$

where ρ_a and T_a correspond to the air density and temperature at the forcing atmospheric level, c_p is the specific heat of dry air, and $RESA_g$ is the aerodynamical surface resistance of the bare ground given by $(C_{Hg} V_a)^{-1}$ where C_{Hg} is the turbulent exchange coefficient for heat over bare ground and V_a is wind speed at the lowest atmospheric level. It should be mentioned that a minimum value for V_a is enforced in SVS (as it was for ISBA). Also, the exchange coefficient C_{Hg} is calculated using roughness lengths representative of both the entire model grid area (for momentum fluxes) and the bare ground (for thermal fluxes). The latent heat of evaporation from the bare ground is $LE_g = \rho_a L_{eff} E_g$, where E_g is the bare ground water vapor flux and L_{eff} is the *effective* latent heat. Effective latent heat is computed to account for the sublimation of ice in the soil, and is defined as follows:

$$L_{eff} = f_{ice} L_i + (1 - f_{ice}) L_v \tag{62}$$

in which

$$f_{ice} = \frac{w_{f\,\mathrm{int}}}{w_{f\,\mathrm{int}} + w_{\mathrm{int}}} \tag{63}$$

is the fraction of ice in the intermediate soil layer defined above, and L_i and L_v are the latent heat of sublimation and evaporation respectively. The bare ground vapor flux is:

$$E_g = \frac{HR_g\, q_{sat}(T_{Gs}) - q_a}{RESA_g} \tag{64}$$

where HR_g is a "relative humidity" of bare ground, $q_{sat}(T_{Gs})$ is the saturated specific humidity of air near bare ground at temperature T_{Gs}, and q_a is the atmospheric specific humidity at the lowest model level. If the bare ground vapor flux is negative because the low level air is more moist *i.e.*, $q_a > q_{sat}(T_{Gs})$, then the E_g is set to zero. The relative

humidity HR_g of the bare ground surface is related to the superficial soil moisture w_1 following

$$HR_g = \begin{cases} \frac{1}{2}\left[1.0 - \cos\left(\frac{w_1}{w_{fc}}\pi\right)\right] & \text{if} \quad w_1 < w_{fc} \\ 1 & \text{if} \quad w_1 \geq w_{fc} \end{cases} \tag{65}$$

where w_{fc} is volumetric water content at the field capacity (Noilhan and Planton 1989). It can be seen in (65) that when the soil is very humid, it is assumed that the humidity of the bare ground surface is equivalent to a saturated surface (similar to a water surface). In case of dew flux when $q_{sat}(T_{Gs}) < q_a$, HR_g is also set to 1.0 (see Mahfouf and Noilhan 1991 for details).

In (56), $freez_g$ and $melt_g$ are the fluxes associated with the freezing and melting of soil water. Based on Giard and Bazile (1999), these fluxes are proportional to differences between the soil surface (T_s) and the freezing / melting temperatures (i.e., T_0=273.16 K):

$$freez_g = \rho_w d_{\text{int}} K \left(\frac{w_{\text{int}}}{w_{sat\,\text{int}}}\right)^{b_{freez}} (T_0 - T_s) \quad \text{with} \quad 0 \leq freez_g \tag{66}$$

$$melt_g = \rho_w d_{\text{int}} K (T_s - T_0) \quad \text{with} \quad 0 \leq melt_g \tag{67}$$

where ρ_w is the water density, d_{int} is the depth of the intermediate soil layer used for melting and freezing processes, K=1.0x10^{-6}, and b_{freez}=4.0 is a coefficient used to control the freezing rate of soil water in the model. For simplicity's sake, the temperature of the superficial soil layer (T_s) is now approximated by taking a coverage-weighted mean of the bare ground skin temperature (T_{Gs}), the mean vegetation temperature (T_{Vd}), the mean snow temperature (T_{SNd}), and the mean SVH (T_{SVd}) temperatures:

$$\begin{aligned} T_s = {} & \overbrace{\left(1 - v_{low} - v_{high}\right)\left(1 - p_{sn}\right)T_{Gs}}^{\text{bare ground}} + \overbrace{\left(1 - v_{high}\right) p_{sn}\, T_{SNd}}^{\text{snow}} + \overbrace{p_{svh} v_{high}\, T_{SVHd}}^{\text{SVH}} \\ & + \overbrace{\left(v_{low}\left(1 - p_{sn}\right) + v_{high}\left(1 - p_{svh}\right)\right)T_{Vd}}^{\text{vegetation}} \end{aligned} \tag{68}$$

rather than a more physical solution. The associated mean soil temperature (T_d) (representative of temperature at a deeper soil depth, approximately 10-20 cm below the soil surface) is a prognostic variable computed using the force-restore method (with only the restore term):

$$\frac{\partial T_d}{\partial t} = \frac{1}{\tau}(T_s - T_d)\,. \tag{69}$$

Equations for the other temperatures, T_{SNd}, T_{SVHd}, and T_{Vd}, are discussed in the sections below.

G. Snow

Two distinct snow packs are considered in SVS: one overlaying bare ground and low vegetation, and the other under high vegetation. While each of these two snow packs evolve separately, the physical equations describing their evolution are for the most part identical as will be described below. For brevity's sake, the subscript "*SN*" refers to snow over bare ground and low vegetation, and the subscript "*SVH*" to snow under high vegetation.

The prognostic equations for the superficial and mean snow temperatures (T_{Xs} and T_{Xd}, with X= *SN* or *SVH*) are obtained from the force-restore method following:

$$\frac{\partial T_{Xs}}{\partial t} = C_X(R_X - H_X - LE_X) + C_X L_f(freez_X - melt_X - melt_{Xrain}) - \frac{2\pi}{\tau}(T_{Xs} - T_{Xd}) \tag{70}$$

$$\frac{\partial T_{Xd}}{\partial t} = \frac{1}{\tau}(T_{Xs} - T_{Xd}) \tag{71}$$

in which C_X is a thermal coefficient, R_X, H_X, LE_X are the net radiation, sensible heat and latent heat fluxes over the appropriate snow canopy, and $freez_X$, $melt_X$ and $melt_{Xrain}$ are the fluxes of freezing, melting of snow, and melting of snow due to incident rain respectively. The thermal coefficient of snow is given by:

$$C_X = 2\left(\frac{\pi}{\lambda_X c_X \tau}\right)^{\frac{1}{2}} \tag{72}$$

where $\lambda_X = \lambda_i(\rho_X / p_w)^{1.88}$ (Yen 1981) and $c_X = c_i(\rho_X / \rho_i)$ are the appropriate snow thermal conductivity and heat capacity respectively, in which ρ_X is the snow density, λ_i =2.22 W(K m)$^{-1}$, c_i =2.106x10^3 J (kg K)$^{-1}$, and ρ_i = 900 kg m^{-3} are the constant thermal conductivity, heat capacity, and density of ice, respectively.

The net radiation for the *SN* canopy is given by:

$$R_{SN} = (1-\alpha_{SN})F_{SS}^{-} + \varepsilon_S(F_{SI}^{-} - \sigma_{SB}T_{SNs}^4) \tag{73}$$

where α_{SN} is the albedo of the *SN* canopy and ε_S is the emissivity of snow (constant at 0.97 in SVS). It should be noted that the incoming solar radiation is not split into direct and diffuse components for snow, due to the large uncertainty in specifying corresponding albedos. The *SVH* net radiation balance is modified from (73) to account for partial transmission through the vegetation canopy of both incoming solar radiation and outgoing surface/snow radiation, and for the contribution of high vegetation downward radiant flux to the SVH energy budget, such that:

$$R_{SVH} = \tau_{VH}(1-\alpha_{SVH})F_{SS}^{-} + \chi\varepsilon_S(F_{SI}^{-} - \sigma_{SB}T_{SVHs}^4) + (1-\chi)\sigma_{SB}T_{Vs}^4 \tag{74}$$

in which

$$\tau_{vh} = \exp\left(-\frac{LAI_{vh}}{2\cos(\phi_L)}\right) \tag{75}$$

is the canopy transmissivity for high vegetation (Sicart, 2004), in which LAI_{vh} is the leaf area index aggregated over high vegetation types only, ϕ_L is the solar angle, and

$$\chi = \exp(-LAI_{vh}) \tag{76}$$

is the skyview factor for high vegetation, roughly approximated from Versheghy et al. (1993) who used $\exp(-0.5LAI_{vh})$ and $\exp(-1.5LAI_{vh})$ for needleleaf and broadleaf trees, respectively. It should be noted that there is a (small) inconsistency in the current formulation of the scheme because the outgoing radiant snow energy that is in theory intercepted by high vegetation ($(1-\chi)\varepsilon_S(\sigma_{SB}T_{SVHs}^4)$) is not considered in the vegetation energy budget.

The sensible heat flux over snow is:

$$H_X = \frac{\rho_a c_p (T_{Xs} - T_a)}{RESA_X} \tag{77}$$

where T_{Xs} is the surface snow temperature, and $RESA_X$ is the aerodynamical surface resistance, given by $(C_{HX}V_a)^{-1}$ where C_{HX} is the drag coefficient for heat over the appropriate snow canopy. The latent heat of evaporation / sublimation from snow is

$LE_X = \rho_a L_i E_X$, where E_X is the snow water vapor flux. Because snow is always considered as "saturated", the specific humidity of snow is exactly equal to the saturation specific humidity and the snow vapor flux is given by:

$$E_X = \frac{q_{sat}(T_{Xs}) - q_a}{RESA_X} \tag{78}$$

where $q_{sat}(T_{Xs})$ is the saturated specific humidity at temperature T_{Xs}.

The melt and freezing fluxes of snow are given by:

$$freez_X = \frac{(T_0 - T_{Xs})}{C_X L_f \Delta t} \quad \text{with} \quad 0 \le freez_X \le \frac{W_{LX}}{\Delta t} \tag{79}$$

$$melt_X = \frac{(T_{Xs} - T_0)}{C_X L_f \Delta t} \quad \text{with} \quad 0 \le melt_X \le \frac{W_{SX}}{\Delta t} \tag{80}$$

where Δt is the model timestep, W_{LX} is a prognostic variable for the liquid water content retained in the appropriate snow pack, W_{SX} is the appropriate snow mass (equivalent water content of snow). The melting associated with rain falling on the snow can be written as

$$melt_{Xrain} = f_{rain} \frac{T_{rain} - T_0}{2C_X L_f \Delta t} \tag{81}$$

where T_{rain} is the temperature of the rain falling on the snow (taken to be the low-level air temperature T_a) and f_{rain} is a factor modulating the strength or the rain melt term depending on the intensity of precipitation; if the rain intensity is relatively small, then $f_{rain}=0$, otherwise f_{rain} increases proportionally to the rainrate up to a maximum value of 1.0.

The equivalent water content of the snow reservoir, *i.e.*, the snow mass (W_{SX}), evolves according to:

$$\frac{\partial W_{SX}}{\partial t} = S_R - \rho_w E_X + freez_X - melt_X - melt_{Xrain} \tag{82}$$

where S_R is the snowfall rate and $\rho_w E_X$ represents the sublimation of the appropriate snow surface. The liquid water in the snow pack (W_{LX}) evolves based on:

$$\frac{\partial W_{LX}}{\partial t} = PS_X - RU_X + melt_X - freez_X \tag{83}$$

where PS_X represents the contribution of rain and/or vegetation runoff to W_{LX} and RU_X is the runoff of liquid water from the appropriate snow pack. Depending on the snow pack considered, PS_X is given by:

$$\begin{aligned} PS_{SVH} &= \left(R_R - R_{Rintercepted}\right) + RV \\ PS_{SN} &= R_R \end{aligned} \tag{84}$$

where R_R is the rainfall, $R_{Rintercepted}$ is the portion of the rain rate intercepted by vegetation, and RV is the runoff from the vegetation canopy. The liquid runoff from the vegetation canopy is only considered in the *SVH* case because by definition the entire snowpack is under the vegetation in the *SN* case. When the amount of liquid water in the snow approaches and exceeds a critical water content W_{LXmax}, there is percolation (throughfall) of liquid water towards the ground, following

$$RU_X = \begin{cases} \dfrac{W_{LX}}{\tau_{hour}} \exp\left(W_{LX} - W_{LX\,\max}\right) & if \quad W_L \le W_{LX\,\max} \\ \dfrac{W_{LX\,\max}}{\tau_{hour}} + \dfrac{W_{LX} - W_{LX\,\max}}{\Delta t} & if \quad W_L > W_{LX\,\max} \end{cases} \tag{85}$$

where

$$W_{LX\,\max} = c_X^R W_{SX} \tag{86}$$

in which τ_{hour} is a time constant of one hour and c_X^R is a retention factor depending on the appropriate snow density:

$$c_X^R = \begin{cases} c_{\min}^R & if \quad \rho_X \ge \rho_e \\ c_{\min}^R + \dfrac{\left(c_{\max}^R - c_{\min}^R\right)\left(\rho_e - \rho_X\right)}{\rho_e} & if \quad \rho_X < \rho_e \end{cases} \tag{87}$$

with $c_{\min}^R$ = 0.03, $c_{\max}^R$ = 0.10, and ρ_e = 0.2.

The presence of snow covering the ground and vegetation can greatly influence the energy and mass transfers between the land surface and the atmosphere. Notably, a snow layer modifies the radiative balance at the surface by increasing the albedo. To consider

this effect, the albedo of snow α_X is treated as a prognostic variable. If snow is melting, the albedo decreases linearly with time to a minimum value of $\alpha_{S\min}$=0.5:

$$\alpha_X(t) = \alpha_X(t-\Delta t) - \Delta t\left(\frac{\tau_{melt}}{\tau} - \frac{S_R(\alpha_{S\max} - \alpha_{S\min})}{W_{crn}}\right) \quad with \quad \alpha_X(t) \geq \alpha_{S\min} \tag{88}$$

otherwise, when the snow is "cold", the albedo increases linearly with time:

$$\alpha_X(t) = \alpha_{S\min} + (\alpha_X(t-\Delta t) - \alpha_{S\min})\exp\left(-\Delta t\frac{\tau_{freez}}{\tau}\right) + \Delta t\frac{S_R(\alpha_{S\max} - \alpha_{S\min})}{W_{crn}} \quad with \quad \alpha_X(t) \leq \alpha_{S\max} \tag{89}$$

up to a maximum value of $\alpha_{S\max}$ = 0.8. In this formulation, $\alpha_X(t)$ is the prognostic albedo of the appropriate snow canopy at the current time step, $\alpha_X(t-\Delta t)$ is the snow albedo from the previous time step, τ_{melt}=0.008 and $\tau_{freez} = 0.24$.

The snow density (ρ_X) evolves under the influence of three factors: (1) snowfall, (2) freezing of liquid water in the snow pack, and (3) aging of the snow canopy. These three factors are applied in SVS in a sequential manner. Normally, the density of freshly falling snow is less than that of snow on the ground, with the effect that snowfall reduces the snow density:

$$\rho_X^* = \frac{(W_{SX}^* - S_R\Delta t)\rho_X(t-\Delta t) + S_R\Delta t\rho_{fall}}{W_{SX}^*} \tag{90}$$

where ρ_X^* is an intermediate snow density value after snowfall, $\rho_X(t-\Delta t)$ is the snow density at the previous-timestep, $W_{SX}^* = \max(W_{SX}, S_R\Delta t)$, and ρ_{fall} is an estimate of the density of falling snow given by:

$$\rho_{fall} = 109. + 6.(T_{2m} - T_0) + 26\left(u_a^2 + v_a^2\right)^{\frac{1}{4}} \quad with \quad \rho_{\min} \leq \rho_{fall} \leq 250 kg\ m^{-3} \tag{91}$$

where T_{2m} is the air temperature 2 meters above ground level (AGL), u_a and v_a are the u and v component of the wind at 10 meters, and $\rho_{\min} = 50$ kg m^{-3}. As the snowpack ages, snow settles due to gravity, and the simulated density increases exponentially following:

$$\rho_X^{**} = \begin{cases} \left(\rho_X^* - \rho_{X\max}\right) \exp\left(-\Delta t \dfrac{\tau_{freez}}{\tau}\right) + \rho_{X\max} & if \quad \rho_X^* < \rho_{X\max} \\ \rho_X^* & if \quad \rho_X^* \geq \rho_{X\max} \end{cases} \tag{92}$$

where ρ_X^{**} is an intermediate value of snow density after snow pack aging, and $\rho_{X\max}$ is the maximum snow density of the appropriate snow canopy. The maximum snow density is a diagnostic variable determined this way:

$$\rho_{X\max} = \begin{cases} 450 - \dfrac{20470}{h_X}\left\{1 - \exp\left(\dfrac{h_X}{67.3}\right)\right\} & if \quad melt_X > 0 \\ 600 - \dfrac{20470}{h_X}\left\{1 - \exp\left(\dfrac{h_X}{67.3}\right)\right\} & if \quad melt_X = 0 \end{cases} \tag{93}$$

where h_x is the snow depth (units of cm). Finally, the increase of snow density due to freezing of water in the snow pack is calculated based on the exchange of water between the W_{LX} and W_{SX} reservoirs so that:

$$\rho_X(t) = \left(\frac{W_{SX}}{W_{SX} + freez_X \Delta t}\right)\rho_X^{**} + \left(\frac{freez_X \Delta t}{W_{SX} + freez_X \Delta t}\right)\rho_{ice} \tag{94}$$

where $\rho_X(t)$ is the snow density at time t, and $\rho_{ice} = 900$ kg m^{-3} is the density of pure ice. Based on (94), the snow density can have values much larger than $\rho_{X\max}$, which is normal near the end of the cold season. The snow depth is directly related to the snow density by $h_x = W_{SX} / \rho_X$.

H. Hydrology

As has been shown in Fig 2, the SVS scheme includes N_L number of predefined soil layers. The corresponding prognostic equations for soil moisture volumetric content in the different layers are:

$$\begin{aligned} \frac{\partial w_1}{\partial t} = \frac{1}{\rho_w d_1}\Big\{ & \Big(\left(1 - v_{low} - v_{high}\right)\left(1 - p_{sn}\right)R_r + \left(v_{low}\left(1 - p_{sn}\right) + v_{high}\left(1 - p_{svh}\right)\right)RU_V \\ & + RU_{SN} + RU_{SVH} + melt_g - freez_g - E_g - f_{1,root}E_{tr} - RU_{surf}\Big\} \\ & - K_1 - D_1 \end{aligned} \tag{95}$$

$$\frac{\partial w_n}{\partial t} = \frac{-f_{n,root}}{\rho_w (d_n - d_{n-1})} E_{tr} + \left(\frac{d_{n-1}}{d_n - d_{n-1}} \right) (K_{n-1} + D_{n-1}) - K_n - D_n \quad for \;\; 1 < n < N_L \qquad (96)$$

$$\frac{\partial w_{N_L}}{\partial t} = \frac{-f_{N_L,root}}{\rho_w (d_{N_L} - d_{N_L-1})} E_{tr} + \left(\frac{d_{N_L-1}}{d_{N_L} - d_{N_L-1}} \right) (K_{N_L-1} + D_{N_L-1}) - K_{N_L} \qquad (97)$$

in which w_1, w_2, …. $w_{\rm NL}$ are the mean soil volumetric water contents for the different soil layers, and d_1, d_2, …., $d_{\rm NL}$ are the depths of these layers. Furthermore, RU_V is the water throughfall from the vegetation, and RU_{surf} is the surface flow (or runoff).

For the w_1 evolution, (95) represents the water budget over the soil layer of depth d_1. The first term on the RHS includes the effect of rainfall, throughfall from snow and vegetation, melting/freezing, evaporation, transpiration, and surface flow. The other terms, K_1 and D_1, are respectively for gravitational flow (drainage) and diffusion contributions from the first to the second layer.

The gravitational drainage from any layer n is proportional to the water amount exceeding that at field capacity (i.e., w_n - w_{fc}) (see Mahfouf et al. 1994):

$$K_n = \frac{d_{N_L}}{d_n - d_{n-1}} \frac{C_3}{\tau} \, \mathrm{MAX}\left[0 \, , \, w_n - w_{fc}\right] \qquad (98)$$

in which C_3 is a parameter that depends on soil texture only. The diffusion from the n-th layer is given by:

$$D_n = \frac{C_4}{\tau} (w_n - w_{n+1}) \qquad (99)$$

where the new parameter C_4 has been calibrated against multilayer soil hydrological models, and is expressed following:

$$C_4 = \frac{d_{n+1} - d_n}{d_{n+1} - d_{n-1}} \; C_{4ref} \; \overline{w}_{n,n+1}^{C_{4b}} \qquad (100)$$

with the $C_{4\rm ref}$ and $C_{4\rm b}$ parameters being functions of the soil texture, and the layer-averaged soil water content is given by:

$$\overline{w}_{n,n+1} = \left\{ \left(\frac{d_n - d_{n-1}}{d_{n+1} - d_{n-1}} \right) w_n^q + \left(\frac{d_{n+1} - d_n}{d_{n+1} - d_{n-1}} \right) w_{n+1}^q \right\}^{1/q} \qquad (101)$$

A value of 6 is used for the exponent q. Based on Boone et al. (1999), this value was determined by carrying out numerous numerical simulations and then comparing

diffusion between a multilayer soil model and ISBA-3L (the 3-layer version of ISBA force-restore at Meteo-France). As the soil moisture gradient increases, the layer-averaged water content used to evaluate the diffusion restore coefficient (C_4) is increasingly weighted by the value of the wettest of the two subsurface soil layers.

For the last layer (i.e. layer N_L), the first term on the RHS represents loss of water due to evapotranspiration (based on the fraction of roots in this layer), the second term is for the exchange with the layer above it due to gravitational and diffusive flows, and the third term is the base flow, i.e., loss due to gravitational flow at the base of the layer.

The temporal evolution of volumetric water content of frozen soil water (i.e., w_f) is represented in SVS using the following equation:

$$\rho_w d_1 \frac{\partial w_f}{\partial t} = freez_g - melt_g \,. \tag{102}$$

And the final "reservoir" that is part of SVS's simulated water budgets, the water content W_r of liquid water in the vegetation canopy, is forced by formation of dew and by interception of rainfall. This water evaporates in the air at a potential rate from the fraction δ [see (16)] of the foliage covered with a film of water, as the remaining part 1-δ of the leaves transpires. Following Deardorff (1978),

$$\frac{\partial W_r}{\partial t} = \left(v_{low}\left(1-p_{sn}\right)+v_{high}\left(1-p_{svh}\right)\right)R_r-\left(E_V-E_{tr}\right)-RU_V \quad with \quad 0 \le W_r \le W_{\max} \tag{103}$$

where, as in previous equations, E_V is the evaporation from the vegetation including the transpiration E_{tr} and the direct evaporation E_d when positive, and the dew flux when negative (in this case E_{tr} = 0), and W_{rmax} is the same as in (17).

Runoff in SVS is based on the Variable Infiltration Capacity (VIC) model (Wood et al. 1992, Habets et al. 1999), and is given by

$$RU_{surf} = RU_g - \frac{i_m}{B+1}\left\{\left(1-\frac{i_o}{i_m}\right)^{B+1} - \left(1-\frac{i_o}{i_m}-\frac{RU_g}{i_m}\right)^{B+1}\right\} \tag{104}$$

in which RU_{surf} is the surface runoff accumulated over a single time step, RU_g is the liquid water reaching the surface (from rainfall or throughfall from vegetation or snow

melt) during the same time step, B is a form parameter to be calibrated, i_m is the maximum infiltration capacity, given by

$$i_m = (1+B) w_{sat} d_{int} \tag{105}$$

and i_o is the infiltration capacity, given by

$$\frac{i_o}{i_m} = 1 - \left(1 - \frac{w_{int} + w_{fint}}{w_{sat}}\right)^{\frac{1}{1+B}} \tag{106}$$

To circumvent problems related to the intensity of the surface runoff, a time step value of 3600s is used for RU_{surf} and RU_g (with renormalization to the model time step Δt). These values are consistent with those used in the VIC model.

I. Grid-scale mean values

For the net radiation flux R_{surf}, the net sensible heat flux H_{surf}, the total latent heat flux of evaporation LE_{surf}, the total water vapor flux E_{surf}, the mean surface albedo α_{surf}, and the mean skin temperature T_{surf}, the spatial averaging is done using an area-of-coverage weighted mean:

$$X_{surf} = \overbrace{(1-v_{low}-v_{high})(1-p_{sn})X_G}^{\text{bare ground}} + \overbrace{(1-v_{high})\,p_{sn}\,X_{SN}}^{\text{snow}} + \overbrace{p_{svh\_a} v_{high}\,X_{SVH}}^{\text{SVH}} + \overbrace{\left(v_{low}(1-p_{sn}) + v_{high}(1-p_{svh\_a})\right)X_V}^{\text{vegetation}} \tag{107}$$

where X_{surf} is the appropriate aggregate surface variable; and X_G, X_V, X_{SN} and X_{SVH} are the corresponding bare ground, vegetation, snow, and snow-under-high-vegetation variables, respectively. It should be noted that the p_{svh_a} snow fraction is used for this aggregation, which is done from the point of view of the atmosphere (in relation with the atmospheric model GEM).

For surface humidity, the following equation is used:

$$q_{surf} = \overbrace{\left(1-v_{low}-v_{high}\right)\left(1-p_{sn}\right)hr_g\, q_{sat}\left(T_{Gs}\right)}^{bare\ ground} + \overbrace{\left(1-v_{high}\right)p_{sn}\, q_{sat}\left(T_{SNs}\right)}^{snow} + \overbrace{p_{svh\_a}v_{high}\, q_{sat}\left(T_{SVHs}\right)}^{SVH} + \overbrace{\left(v_{low}\left(1-p_{sn}\right)+v_{high}\left(1-p_{svh\_a}\right)\right)\left(h_V\, q_{sat}\left(T_{Vs}\right)+\left(1-h_V\right)q_a\right)}^{vegetation} \tag{108}$$

J. Surface boundary conditions for vertical diffusion

In current versions of SVS and GEM, the surface schemes interact with the overlying atmosphere through GEM's vertical diffusion. The surface schemes (including SVS) provide the lower boundary condition to the following diffusion equations:

$$\frac{\partial\theta}{\partial t} = \frac{1}{\rho}\frac{\partial}{\partial z}\left(\rho K_T \frac{\partial\theta}{\partial z}\right) = -\frac{1}{\rho}\frac{\partial}{\partial z}\rho\,\overline{w'\theta'} \tag{109}$$

$$\frac{\partial q}{\partial t} = \frac{1}{\rho}\frac{\partial}{\partial z}\left(\rho K_T \frac{\partial q}{\partial z}\right) = -\frac{1}{\rho}\frac{\partial}{\partial z}\rho\,\overline{w'q'} \tag{110}$$

$$\frac{\partial \mathbf{V}}{\partial t} = \frac{1}{\rho}\frac{\partial}{\partial z}\left(\rho K_M \frac{\partial \mathbf{V}}{\partial z}\right) = -\frac{1}{\rho}\frac{\partial}{\partial z}\rho\,\overline{w'\mathbf{V}'} \tag{111}$$

As part of the numerical solution of these equations, the lower boundary conditions can be written in this manner:

$$-\left(\overline{w'\theta'}\right)_S = \alpha_\theta + \beta_\theta\,\theta^+_{NK\_atm} \tag{112}$$

$$-\left(\overline{w'q'}\right)_S = \alpha_q + \beta_q\, q^+_{NK\_atm} \tag{113}$$

$$-\left(\overline{w'\mathbf{V}'}\right)_S = \alpha_V + \beta_V\, \mathbf{V}^+_{NK\_atm} \tag{114}$$

Making the link with the fluxes calculated in SVS, based on the similarity theory applied to the atmospheric surface layer:

$$\left(\overline{w'\theta'}\right)_S = C_T\, u_*\left[\theta^+_S - \left(1-f_S\right)\theta_{NK\_atm} - f_S\,\theta^+_{NK\_atm}\right] \tag{115}$$

$$\left(\overline{w'q'}\right)_S = C_T\, u_* \left[q_S^+ - (1 - f_S) q_{NK\_atm} - f_S\, q_{NK\_atm}^+\right] \tag{116}$$

$$\left(\overline{w'\mathbf{V}'}\right)_S = C_M\, u_*\, \mathbf{V}_{NK\_atm}^+\, \mathbf{V}_{NK\_atm}^+ \tag{117}$$

in which f_S indicates whether the lower boundary condition is implicit (f_S=1) or explicit (f_S=0).

The α and β coefficients then become:

$$\alpha_\theta = -C_T\, u_* \left[\theta_S^+ - (1 - f_S)\theta_{NK\_atm}\right] \quad \text{and} \quad \beta_\theta = -C_T\, u_*\, f_S \tag{118}$$

$$\alpha_q = -C_T\, u_* \left[q_S^+ - (1 - f_S) q_{NK\_atm}\right] \quad \text{and} \quad \beta_q = -C_T\, u_*\, f_S \tag{119}$$

$$\alpha_V = 0 \quad \text{and} \quad \beta_q = -C_M\, u_* \left|\mathbf{V}\right| \tag{120}$$

It should be noted that in the explicit case, the α coefficients are exactly the surface fluxes of temperature and humidity, which can be derived from an aggregation of the subgrid-scale components. Unfortunately, using an explicit boundary condition at the surface often leads to numerical instabilities. For this reason the implicit treatment is the default option in SVS and GEM. The price to pay for this numerical stability is a slight inconsistency between the amount of heat and humidity calculated in SVS and the amount received by the atmosphere.

K. Upcoming developments

There are several aspects of SVS that are currently being improved:

- representation of subgrid-scale variability for the calculations related with the surface / atmospheric turbulent fluxes,
- vertical transport of soil water based on diffusion theory;
- inclusion of subsurface / lateral flow and base flow (drainage) based on subgrid-scale slope information,
- vertical transport of heat in the soil, using K-diffusion, and including the two snow packs;

- improved treatment of F/T state of the soil,
- inclusion of interception of snow by vegetation.

APPENDIX A: Numerical solution of the Force-Restore equation for surface temperature.

The Force-Restore equation for the surface temperatures of bare ground, vegetation, and snow, has the form:

$$\frac{\partial T_s}{\partial t} = C\left[R_n - H - LE\right] - \frac{2\pi}{\tau}\left[T_s - T_d\right] \tag{A1}$$

where T_s is the surface (skin) temperature (of bare ground, vegetation, or snow), C is a thermal coefficient, R_n is the net radiation, H is the sensible heat flux, LE is the latent heat flux, τ is a time constant of one day, and T_d is the mean surface temperature.

The net radiation is given by:

$$R_n = F_{S\downarrow}\left(1-\alpha\right) + F_{L\downarrow} - \varepsilon\sigma T_s^4 \tag{A2}$$

in which $F_{S\downarrow}$ is the total downwelling solar radiation (note that for simplicity this quantity is not split into direct and diffuse components), α is the surface albedo, and $F_{L\downarrow}$ is the downwelling longwave radiation.

The sensible heat flux is given by:

$$H = \rho_a c_p C_T u_* \left(T_s - \theta_a\right) \tag{A3}$$

in which C_T is the coefficient for turbulent exchanges of heat between the surface and the atmosphere, u_* is the friction velocity, and θ_a is the air potential temperature at the lowest atmospheric model (on which temperature is defined).

The latent heat flux is given by:

$$LE = \rho_a L C_T u_* \left[hu\, q_{sat}(T_s) - q_a\right] \tag{A4}$$

in which hu is the surface "relative humidity", $q_{sat}(T_s)$ is the saturation value of specific humidity for air at temperature T_s, and q_a is the specific humidity at the lowest atmospheric level (on which specific humidity is defined – same as air temperature).

Following this, and considering temporal discretization, (A1) can be rewritten as follows:

$$\frac{T_s^+ - T_s^-}{\Delta t} = C\left\{F_{S\downarrow}(1-\alpha) + F_{L\downarrow} - \varepsilon\sigma T_s^{+4} - \rho_a c_p C_T u_* \left(T_s^+ - \theta_a\right) - \rho_a L C_T u_* \left[hu\, q_{sat}\left(T_s^+\right) - q_a\right]\right\}$$

$$-\frac{2\pi}{\tau}\left(T_s^+ - T_d\right) \tag{A5}$$

Proceeding with a linearization of the type:

$$f\left(T_s^+\right) = f\left(T_s\right) + \left(T_s^+ - T_s\right) f'\left(T_s\right) \tag{A6}$$

we get:

$$\varepsilon\sigma T_s^{+4} \approx \varepsilon\sigma\left[T_s^{-4} + 4\left(T_s^+ - T_s^-\right)T_s^{-3}\right] \tag{A7}$$

$$q_{sat}\left(T_s^+\right) \approx q_{sat}\left(T_s^-\right) + \left(T_s^+ - T_s^-\right)\frac{\partial q_{sat}\left(T_s^-\right)}{\partial T} \tag{A8}$$

Going back to (A5), we have the full equation to solve for T_s^+:

$$\frac{T_s^+ - T_s^-}{\Delta t} = C\left\{F_{S\downarrow}(1-\alpha) + F_{L\downarrow} - \varepsilon\sigma\left[T_s^{-4} + 4\left(T_s^+ - T_s^-\right)T_s^{-3}\right]\right.$$

$$\left. - \rho_a c_p C_T u_* \left(T_s^+ - \theta_a\right) - \rho_a L C_T u_* \left[hu\, q_{sat}\left(T_s^-\right) + hu\left(T_s^+ - T_s^-\right)\frac{\partial q_{sat}\left(T_s^-\right)}{\partial T} - q_a\right]\right\}$$

$$-\frac{2\pi}{\tau}\left(T_s^+ - T_d\right) \tag{A9}$$

REFERENCES

Arora, V. K. and G. J. Boer, 2003. Simulating energy and carbon fluxes over winter wheat using coupled land surface and terrestrial ecosystem models, Agricultural and Forest Meteorology, 118 (1-2), 21-47.

Arora, V. K, and G. J. Boer, 2012. The Canadian terrestrial ecosystem model (CTEM) v1.0 and v1.1.Bélair, S., L.-P. Crevier, J. Mailhot, B. Bilodeau, and Y. Delage, 2003a: Operational implementation of the ISBA land surface scheme in the Canadian regional weather forecast model. Part I: Warm season results. J. Hydromet., 4, 352-370.

Ball, J. T., I. E. Woodrow, and J. A. Berry, 1987. A model predicting stomatal conductance and its contribution to the control of photosynthesis under different environmental conditions, in Progress in Photosynthesis Research, edited by J. Biggens, Dordrecht, Martinus Nijhoff. IV, 221-224.

Bélair, S., R. Brown, J. Mailhot, B. Bilodeau, and L.-P. Crevier, 2003b: Operational implementation of the ISBA land surface scheme in the Canadian regional weather forecast model. Part I: Cold season results. J. Hydromet., 4, 371-386.

Bélair, S., M. Roch, A.-M. Leduc, P.A. Vaillancourt, S. Laroche, and J. Mailhot, 2009: Medium-range quantitative precipitation forecasts from Canada's new 33-km deterministic global operational system. Wea. Forecasting, 34, 690-708.

Bhumralkar, C.-M., 1975 : Numerical experiments on the computation of ground surface temperature in an atmospheric general circulation model. J. Appl. Meteorol. , 14, 1246-1258.

Blackadar, A.-K., 1976: Modeling the nocturnal boundary layer. Proc. Third Symp. On Atmospheric Turbulence, Diffusion and Air Quality , Boston, Amer. Meteor. Soc., 46-49.

Boone, A., J.-C. Calvet, and J. Noilhan, 1999: Inclusion of a third soil layer in a land surface scheme using the Force–Restore method. J. Appl. Meteorol., 38, 1611-1630.

Braud, I., J. Noilhan, P. Bessemoulin, P. Mascart, R. Haverkamp, and M. Vauclin, 1993: Bare-ground surface heat and water exchanges under dry conditions: Observations and parameterization. Bound.-Layer Meteror., 66, 173-200.

Collatz, G. J., J. T. Ball, C. Grivet, and J. A. Berry, 1991. Physiological and environmental regulation of stomatal conductance, photosynthesis, and transpiration: a model that includes a laminar boundary layer. Agricultural and Forest Metoerology, 54, 107-136.

Collatz, G. J., M. Ribas-Carbo, and J. A. Berry, 1992. Coupled photosynthesis-stomatal conductance model for leaves of plants. Aust. J. Plant Physiol., 19, 519-538.

Deardorff, J.W., 1977: A parameterization of ground surface moisture content for use in atmospheric prediction models. J. Appl. Meteor., 16, 1182-1185.

Deardorff, J. W., 1978: Efficient prediction of ground surface temperature and moisture with inclusion of a layer of vegetation. J. Geophy. Res., 83, 1889-1903.

Douville, H., 1994: Développement et validation locale d'une nouvelle paramétrisation du manteau neigeux. Note 36 GMME/Météo-France.

Dickinson, R.E., 1984: Modeling evapotranspiration for three dimensional global climate models. Climate Processes and Climate Sensitivity. Geophys. Monogr., 29, 58-72.

Douville, H., J.-F. Royer, and J.-F. Mahfouf,1995: A new snow parameterization for the French community climate model. Part I: Validation in stand-alone experiments. Climate Dyn., 12, 21-52.

Farquhar, G. D., S. von Caemmere, and J.A. Berry, 1980. A biochemical model of photosynthetic assimilation in leaves of species. Planta, 149, 78-90.

Giard, D., and E. Bazile, 2000: Implementation of a new assimilation scheme for soil and surface variables in a global NWP model. Mon. Wea. Rev., 128, 997–1015.

Giordani, H., 1993: Expériences de validation unidimensionnelles du schéma de surface NP89 aux normes Arpège sur trois sites de la campagne EFEDA 91. Note de travail 24 GMME/Météo-France.

Habets, F., and J. Noilhan, 1996: Resultats des simulations d'ISBA dans la phase PILPS2c: Bilan hydrique du bassin de l'Arkansas. CNRM/Meteo-France, note de centre 50.

Habets, F., Noilhan, J., Golaz, C., Goutorbe, J.P., Lacarrre, P., Leblois, E., Ledoux, E., Martin, E., Ottle´, C., Vidal-Madjar, D., 1999. The ISBA surface scheme in a macroscale hydrological model, applied to the HAPEX-MOBILHY area: Part 1 model and data base. J. Hydrol. 217, 75– 96.

Jacquemin, B., and J. Noilhan, 1990: Validation of a land surface parameterization using the HAPEX-MOBILHY data set. Bound.-Layer Meteor., 52, 93-134.

Jarvis, P.G., 1976: The interpretation of the variations in leaf water potential and stomatal conductance found in canopies in the field. Phil. Trans. Roy. Soc. London, B273, 593-610.

Leuning, R., 1995. A critical appraisal of a combined stomatal-photosynthesis model for plants. Plant, Cell and Environment, 18, 339-355.

Mahfouf, J.-F., and J. Noilhan, 1991: Comparative study of various formulations of evaporation from bare soil using in situ data. J. Appl. Meteor., 9, 1354-1365.

Mahfouf, J.-F., J. Noilhan, and P. Péris, 1994: Simulations du bilan hydrique avec ISBA: Application au cycle annuel dans le cadre de PILPS. Atelier de modélisation de l'atmosphère, CNRM/Météo-France, December 1994, Toulouse, France, 83-92.

Noilhan, J., and S. Planton, 1989: A simple parameterization of land surface processes for meteorological models. Mon. Wea. Rev., 117, 536-549.

Noilhan, J., and P. Lacarrère, 1995: GCM grid-scale evaporation from mesoscale modeling. J. Climate, 8, 206-223.

Pons, T. L., and R. A. M. Welschen, 2003. Midday depression of net photosynthesis in the tropical rainforest tree Eperua grandiflora: contributions of stomatal and internal conductances, respiration and Rubisco functioning, Tree Physiology, 23(14), 937-947.

Sellers, P.J., Y. Mintz, Y.C. Sud, and A. Dalcher, 1986: The design of a Simple Biosphere model (SiB) for use within general circulation models. J. Atmos. Sci., 43, 505-531.

Sellers, P. J., J. A. Berry, G. J. Collatz, C. B. Field, and F. G. Hall, 1992. Canopy reflectance, photosynthesis, and transpiration III. A reanalysis using improved leaf models and a new canopy integration scheme. Remote Sens. Environ., 42, 187-216.

Sellers, P. J., 1985. Canopy reflectance, photosynthesis, and transpiration. Int. J. Remote Sensing, 6(8), 1335-1372.

Schenk, H. J., and R. B. Jackson. 2003. Global Distribution of Root Profiles in Terrestrial Ecosystems. Data set. Available on-line [http://www.daac.ornl.gov] from Oak Ridge National Laboratory Distributed Active archive Center, Oak Ridge, Tennessee, U.S.A. doi:10.3334/ORNLDAAC/660.

Sicart, J.E., J.W. Pomeroy, R.L.H. Essery, J. Hardy, T. Link, and D. Marks, 2004: A sensitivity study of daytime net radiation during snowmelt to forest canopy and atmospheric conditions. J. Hydromet., 5, 774-784.

Summer, M.E., 2000: Handbook of Soil Science. CRC Press,. Boca Raton, FL, 2000. 2313pp.

Thompson, N., Barrie, and M. Ayles (1981): The Meteorological Office Rainfall and Evaporation Calculation System: MORECS. Hydrological Memorendum, 45, 69pp.

Verseghy, D. L., 1991: CLASS - A Canadian land surface scheme for GCMs. Part I: Soil model. Int. J. Climatol., 11, 111-133.

Verseghy, D.L., N.A. McFarlane, and M. Lazare, 1993: Class—A Canadian land surface scheme for GCMS, II. Vegetation model and coupled runs. Int. J. Climatol., 13, 347-370.

Wood, E., D. Lettenmaier, and V. Zartarian, 1992: A land-surface hydrology parameterization with subgrid variability for general circulation models. J. Geophys. Res., 97, 2717-2728.

Xu, L., and D. D. Baldocchi, 2003. Seasonal trends in photosynthetic parameters and stomatal conductance of blue oak (Quercus douglasii) under prolonged summer drought and high temperature, Tree Physiology, 23(13), 865-877.

Yen, Y., 1981: Review of thermal properties of snow, ice and sea-ice. CRREL Rep, 81-10.